ALEPH 94-129
PHYSIC 94-113
J.M. Scarr
22.07.1994

Determination of Properties of Quark- and Gluon- Jets without Tagging.

J. M. Scarr
(scarr @ uk.ac.gla.ph.v2)

Glasgow University

14 July 1994

Abstract

Distributions of particle multiplicity, jet masses, etc., and energy distributions within jets have been determined for quark- and gluon- jets using data from two specific three- jet topologies with pairs of equal energy jets. The method used is an alternative to the use of lepton- or vertex- tagging to identify the quark jets and gives the advantage of increased statistical accuracy.

Introduction.

The reaction $e^+e^- \Rightarrow Z \Rightarrow hadrons$ as observed at LEP at energies $\sqrt{S} \approx M_Z$ is ideal for the study of the differences of the properties of quark- and gluon- jets: the cross section is much larger and the jets better defined or more collimated than at previously available energies (e.g. PETRA, $\sqrt{S} \approx 40$ GeV/c²). The three jet topology can be defined to represent $q\bar{q}g$ production since the initial Z decay is $Z \Rightarrow q\bar{q}$ and the additional jet is the consequence of hard gluon radiation. Some scheme such as tagging or energy ordering has to be used to separate the quark- and gluon- jets. It is only recently that clear evidence for difference of quark- and gluon- jets has been given [OPAL: Z. f Physik C58 (93), 387], earlier results at lower energies gave conflicting results. Quite recently indeed, observations consistent with no evidence for differences have been reported [OPAL: P.L. B265 (91), 462] and [DELPHI: Z. f Physik C56 (92), 63]. Thus further examination of quark- and gluon- jet differences is still of interest.

This note presents results obtained using a method, described in the next section, differing completely from those used elsewhere. It is hoped that this new approach will complement the more conventional methods.

Analysis Method

In the following section we describe a method to obtain the properties of quark- and gluon- jets without the use of quark tagging. This procedure allows the use of all events of the desired jet topology (and all quark flavors) and complements the normal tagging approach.

A single jet variable, such as multiplicity or jet mass etc., will be expected to have a different distribution for quark- and gluon- jets. The distributions will be characterised by the number of events in bin i, q_i for quark jets and g_i for gluon jets, where, for a total number of events N, we choose normalisation $\sum q_i = \sum g_i = N$. We select three- jet events with two jets of essentially equal energy. The pair of equal energy jets will be either a $q\bar{q}$ pair or a qg pair (it is assumed that there are no gg pairs; an essential for this method). We then plot a folded scatter plot of the variable for one jet versus the same variable for the other jet of the pair. The plot is folded because we are unable to distinguish the two jets without tagging. The expected distribution of the folded scatter plot is

$$n_{ij} = \{(q_i g_j + g_i q_j)(1-\delta) + 2\delta q_i q_j\} / N$$

where $\delta =$ the fraction of $q\bar{q}$ events in the N event 2- jet sample. Here we have made the assumption (to be relaxed below) that the distributions of the two jets are uncorrelated. If we now write

$$p_i = g_i(1-\delta) + \delta q_i$$

then the scatter plot distribution becomes

$$n_{ij} = (p_i q_j + q_i p_j) / N$$

or with definitions

$$s_i = p_i + q_i$$
$$d_i = p_i - q_i$$

finally,

$$n_{ij} = (s_i s_j - d_i d_j) / 2N + C_{ij}$$

Here the extra term C_{ij} allows for a correlation between the distributions of the two jets, where

$$\sum_i C_{ij} = \sum_j C_{ij} = 0.$$

This final form is the most convenient both conceptually and for fitting the data.

The addition of the correlation term makes the solution ambiguous. The ambiguity is avoided by performing the fit assuming that the correlation term $C_{ij} = 0$ (If a significant correlation actually exists then a poor fit is obtained and the existence of a correlation is revealed). Note that s_i is the projection of the folded scatter plot and hence known; further $\sum d_i = 0$, therefore if each distribution (q and g) consists of M bins, the number of parameters to be fitted is M-1. Thus since the scatter plot has M(M+1)/2 independent bins, the number of degrees of freedom in the fit is M(M-1)/2+1 and is large.

In addition, the final equation shows that reversing the sign of all d_i leaves n_{ij} unaffected. This is equivalent to an ambiguity between p_i and q_i which is the result of the method never making use of jet tagging to identify the quark jet(s). This ambiguity must be resolved before subtraction can be made using a known value of δ to obtain the gluon distribution g_i.

The fit is performed by a Maximum Likelihood search procedure where the likelihood function used is (actually each event is counted twice, hence $2L$).

$$2L = \sum_{ij} D_{ij} \ln\left(1. - \frac{d_i d_j}{s_i s_j}\right)$$

where D_{ij} is the contents of bin ij (see appendix for details). A binned Maximum Likelihood method is used thus avoiding the need for a parameterisation of the distributions which is a priori unknown.

Before the fit the d_i are set equal zero and a chi- square goodness of fit calculated. After optimisation of the d_i the goodness of fit is recalculated. Normally, the initial fit is extremely poor (quark and gluon distributions are different). After optimisation good fits are always obtained indicating consistency with the absence of significant correlations between the two jets for the variables studied here.

The errors on the fitted results are obtained as follows. We take the fit as representing the true distributions and generate 20 Monte Carlo samples of N events using these distributions. These 20 samples are then treated exactly as the data sample and the statistical errors determined from the variation of the fit results.

It is perhaps worth making a final remark on the correlations between jets mentioned above. By absence of correlations, we mean that for a given event the value of p does not influence the value of q. In another sense a correlation between jets does exist, namely, that if one is a gluon then the other is a quark. This is why the existence of a correlation between p and q leads to an ambiguity in the solution of the fit. However we obtain satisfactory fits assuming p and q to be independent and the validity of the method has been checked using Monte Carlo generated events which are in close agreement with data.

Jet Topologies

In the comparison of gluon- and quark- jet properties we have made use of two three- jet topologies which are commonly used for this purpose.

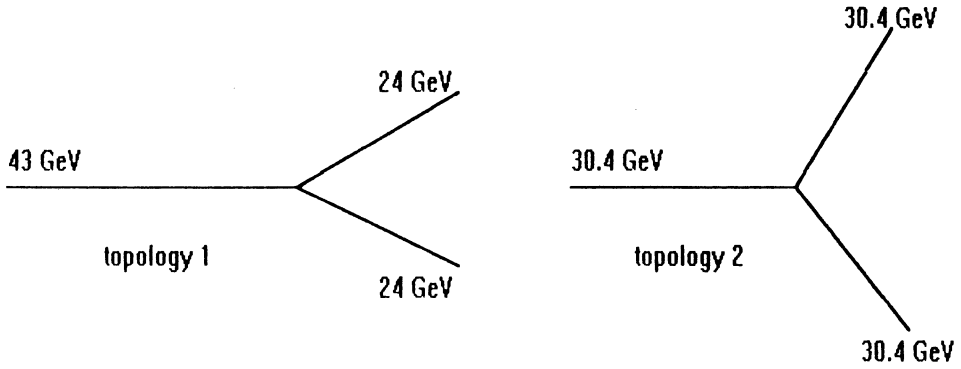

1. The angle between the most energetic jet and each of the other two jets is 150 ± 10 degrees (150 degree sample).

2. The angle between all pairs of jets is 120 ± 20 degrees (120 degree or 'mercedes' sample).

Sample (1) has the advantage of giving a nearly pure qg sample ($\delta \approx 0.03$, estimated from 1st order QCD). The subtraction of the $q\bar{q}$ background is not important (though performed) and a rough estimate of δ is sufficient. Furthermore, the high energy jet gives an almost pure quark- jet sample (the 3% subtraction is not made since the corresponding gluon distribution is unknown). For sample (2) with three equal energy jets, our method is to choose two of the jets at random, hence $\delta = 1/3$ by symmetry. Thus δ is known adequately for each case without the necessity of detailed Monte Carlo studies.

In addition to the angle selection specified above, additional cuts on the jet energies are made as given below (row 5 applies to quark jets only).

	Mean Energy	Energy Range	Aleph Data	Number of Events
1	$\overline{E}$ = 24.4 GeV	$20 < E_{jet} < 29$ GeV	1992 Data	11933 Events
2	$\overline{E}$ = 24.4 GeV	$20 < E_{jet} < 29$ GeV	1993 Data	10651 Events
3	$\overline{E}$ = 24.5 GeV	$22.5 < E_{jet} < 27$ GeV	1992 + 1993 Data	10938 Events
4	$\overline{E}$ = 30.4 GeV	$26 < E_{jet} < 35$ GeV	1992 + 1993 Data	4982 Events
5	$\overline{E}$ = 42.6 GeV	$39.5 < E_{jet} < 44.5$ GeV	1992 Data	11933 Events

It should be noted that the mean energies of the quark- and gluon- jet samples will not be precisely equal due to the energy dependence of the production cross section $d^2\sigma/dx_q dx_g$.

The jets have been found using the particle clustering algorithm PTCLUS which is effectively a jet cone algorithm assigning particles to the jet nearest in angle. A $y_{cut} = 0.03$ (defined as for the Jade algorithm) was used to define the three- jet events and is small enough to include the required topologies. PTCLUS gives a good determination of the jet directions. The best estimate of the jet energies is then determined from the angles between the jets using the formula (which neglects quark masses)

$$E_i^{jet} = \frac{\sin\psi_i}{\sum_{j=1,3} \sin\psi_j} E_{cms}$$

where ψ_i is the angle between the two jets other than jet i.

Details of the event selection are given in an appendix.

Results

Initial Comments.

The results on the properties of quark- and gluon- jet have been obtained from the two three- jet topologies precisely defined in section **Jet topologies.** This exact specification of topology is important, since as well as the jet properties showing dependence on jet energy, their properties may also be dependent on the jet environment or topology of the event The three jet event is taken to be a $q\bar{q}g$ system.

To find the three jet events the algorithm PTCLUS (described in Aleph note no. Aleph 89-150) has been used. Unlike the 'Jade' or 'Durham' algorithms in which two particles or sub- clusters once combined remain permanently so combined, the PTCLUS algorithm, after each merging of sub- clusters, reassigns particles to the jet with the axis to which the particle has the least angle, iterating if necessary. Thus PTCLUS is in effect a type of cone algorithm. This is presumed to be a desirable feature when studying the fraction of energy in cones of various opening angles about the jet axis as is done here.

As explained in section **Analysis Method,** because of our avoidance of tagging quark- jets, there is a fundamental ambiguity which must be resolved before subtraction of quark background from our gluon samples (this ambiguity which exists for each jet variable could be reduced to a single overall ambiguity by studying suitable linear combinations of jet variables). However, we have preferred to resolve this ambiguity for each variable in turn by assuming that gluon jets have the higher multiplicities with consequently softer energy distributions than quark jets, and since the particle transverse momenta relative to the jet axis are fairly similar in the two cases, that gluon jets tend to be broader. We can support this view either on theoretical grounds or with reference to results obtained using tagging of quark jets.

The advantages and differences of not using quark tagging are :

1. All events of the given topology can be used with a consequent gain in statistics. As a result the quark distributions are for the mixture of all quark flavors as produced at the energy of the Z° peak.
2. Quark tagging does not result in pure quark- or gluon- jet samples, and Monte Carlo studies are required to determine the sample purity. Our method avoids the need for such model dependent determinations. It is also possible that tagged quark jets, if used, may result in a quark jet sample differing from that of the totality of quark jets.

We summarise again here the basic features of the method:

1. A folded scatter plot is made of the jet variables for the pairs of jets selected.
2. An initial Chi- square is calculated to determine the goodness of fit for the hypothesis that quark- and gluon- jet distributions are the same. We then

calculate the value of $S = \sqrt{2\chi^2} - \sqrt{2n_f - 1}$, where n_f is the number of degrees of freedom in the fit, and which is approximately normally distributed about zero with standard deviation of one if n_f is large as is the case here. For the 150° sample S lies between 5 and 10 thus excluding this hypothesis. For the smaller 120° sample the rejection of this hypothesis is not so strong, S lies in the range of 1 to 3: nevertheless, fits are obtained which are consistent with the slightly lower energy 150° data.

3. A fit is then made allowing quark- and gluon- distributions to differ. This fit results in an acceptable value for S for all data shown here and is therefore consistent with the assumption of no significant correlation between the distributions of the pairs of jets.
4. The $q\bar{q}$ background is subtracted out after resolving the ambiguity between the initially obtained p- and q- distributions using the definition of p. The ambiguity is resolved with reference to theory and tagged data. In the performance of the background subtraction, the parameter δ (the fraction of $q\bar{q}$ pairs in the sample of jet pairs - see section **Analysis Method**) is either very small and hence does not need to be very accurately determined, or is determined entirely from the symmetry of the event topology. The subtraction implicitly assumes the quark distributions to be identical for $q\bar{q}$ and qg pairs of the given topology. While this assumption is correct for the 120° sample due to the three fold symmetry, it is not necessarily so for the 150° sample as seen by considering the location of the color strings. However, the subtraction in this later case is very small ($\delta \approx 0.03$).
5. The errors on these fits are determined from 20 Monte Carlo samples generated using the obtained quark- and gluon distributions and are statistical only.

The above method has been used on a similar sized sample of Monte Carlo events generated using the Jet Set coherent parton shower program. The results are in close agreement with those obtained from data. Furthermore, with the Monte Carlo events it is possible to examine the parton showers so as to directly identify the quark- and gluon- jets. However, this identification can fail if, for example, a jet includes a large fraction of hadronic energy from more than a single energetic parent parton. In 6% of events it has proved impossible to identify unambiguously the gluon jet using the parton structure of the event. The results from our fitting procedure for the Monte Carlo events have been compared with the 94% of events for which successful parton tagging gives the "true" quark and gluon distributions. The agreement is good (see Aleph meeting on Quark and Gluon Properties - LAPP/Annecy - 21 Feb 94 - Aleph 94-49; M. Scarr, "Unfolding Quark and Gluon Jet Properties") thus supporting the validity of our method.

We show plots of results for the 92 and 93 data separately. The directly observed plot projections $s_i = p_i + q_i = (1+\delta)q_i + (1-\delta)g_i$ (not shown) are closely similar for the two data sets after normalisation. Thus the agreement within errors of our quark- and gluon- distributions for these two data sets supports the correctness of our statistical error estimates.

Using 12000 events we obtain 10% statistical errors over 20 bins for the rather flat distribution of the energy fraction within a 10° cone about the jet axis (see for example figure 1.1). This can be compared with a 4% error which would be expected for pure samples of 12000 quark- and gluon- jets. For comparison, using vertex tagging OPAL obtained 20% errors over 13 bins from a sample (before tagging) of 23000 events; about 140000 events would be required to reduce the errors to our level. Thus an improvement of statistical accuracy is obtained using our unfolding procedure to obtain the properties of quark- and gluon- jets compared to tagging methods.

Data plots.

The set of figures 1.-5. show our main results for 6 variables and 5 selections of data (see **figure captions**). The mean values of these distributions are given in a table. It is quite clear that the properties of quark- and gluon- jets differ significantly and are seen to be generally energy and/or topology dependent. Data sets 1. and 2. allow comparison of 92 and 93 150° data which are in good agreement. However, the mean values for 92 and 93 data differ by more than the statistical errors given. Corresponding slight systematic differences between 92 and 93 data are also observed in the unseparated (sum of the two jets) distributions. The 92 and 93 150° data are from the lower left region of the figure 6 three- jet Dalitz plot in which it can be seen that a correlation exists between the two jet energies. Since jet properties are usually energy dependent, this energy correlation could introduce a correlation between the variables of the two jets although there is no evidence for this in the fits. To reduce this possibility we have combined the 92 and 93 data and imposed tighter energy cuts so that the jet energy ranges are 22.5-26 GeV and 23.5-26 GeV for the lower and upper energy jet respectively. This sample (3.) can be seen to give results consistent with the previous two samples (1. and 2.). The 120° sample (4.) combines the 92 and 93 data. the larger statistical errors for the gluon distributions reflect the larger $q\bar{q}$ subtraction ($\delta = \frac{1}{3}$) for this case. It should be noted that the three- fold symmetry of this configuration has unique implications for the quark and gluon scale factors. Finally, the data for the high energy quark ($\bar{E} \approx$ 43GeV) is shown (.5) and includes an unsubtracted 3% gluon contamination.

For most variables (see table I) the mean values of the distributions increase significantly in going from the 150° ($\bar{E} = 24.4\,GeV$) to the 120° ($\bar{E} = 30.4\,GeV$) sample, a relatively small change of jet energy. Only the mean value of X_E is the same at all energies consistent with the expectations of scaling. The mean fraction of jet energy within a 10° cone (see table I) does not change appreciably between the 150° and 120° data for the equal energy jet pairs although the 43 GeV quark jet does show increased collimation. $\sum|p_t|$ is seen to increase faster than the increase of particle multiplicity indicating an increase of mean particle transverse momentum with increasing energy.

Figures 7 and 8 show distributions for the fraction of jet energy within cones about the jet axis for a range of cone semi- angles for $\bar{E} \approx$ 24.5 GeV (quarks and gluons) and $\bar{E} \approx$ 43 Gev (quarks only, 3% gluon contamination) respectively. The mean fraction of jet energy within these cones is summarised in figure 9a which shows the greater collimation of quark jets compared to gluon jets. Increasing collimation with increasing energy is also indicated. Our data of figure 9a agrees with some preliminary Aleph vertex tagged results shown in figure 9b, though it is not clear yet to what extent agreement should be expected.

Figure 6 shows the regions of the three jet Dalitz plot populated by our two event samples. The full range of the two lower energy 150° sample jets is 20-26 GeV and 23.5-29 GeV for lower and upper energy jets respectively. The upper of these limits overlaps the 120° sample which has significantly different jet properties.

This fact is the motivation for using a tighter energy cut on the 150° sample as mentioned above. It is of interest to note that the appropriate scaling variable for the quark jets is not the jet energy but rather

$$S = \frac{E_q}{E_g}\left(p_q \cdot p_g\right) \approx E_q{}^2\left(1 - \cos\theta_{qg}\right)$$

In this form the angle between the quark- and gluon- jets plays an important role and accentuates the difference between the jets of the 150° and 120° samples above that expected from the energy difference alone. This angular dependence corresponds to a suppression of gluon emission for jets separated by small angles and is the result of an interference effect (intra- jet coherence) between emission by the two jets. In terms of the diagonal axes d_1 and d_2 (see figure 6) variation along the d_2 direction, that is, within the 150° sample, does not influence S greatly. On the other hand, changes in the d_1 direction lead to rapid variation of the angle between the two low energy jets and a consequent large change to S. Moving from the 150° sample to the 120° sample the inter- jet angle increases from 60° to 120° giving a factor of ×3 in the angular factor of S. This behaviour of S may help to explain the differences observed between the two data samples. The behaviour of the gluon jets is dependent on two scales of similar form given by

$$S_q = \frac{E_g}{E_q}\left(p_g \cdot p_q\right)$$

and a corresponding $S_{\bar{q}}$.

The above scale formulae are those used in the Herwig parton shower Monte Carlo where they are responsible for maintaining angular ordering within jets [see CERN 89-08, Vol. 3 p239-240]. Perhaps it is not clear that they can be applied to such large inter- parton angles as occur here, but they serve as a reminder that not only parton energies determine jet characteristics.

8. Summary and Conclusions

We have used events from two well defined three jet topologies to compare the properties of quark- and gluon- jets of equal energies. Definite differences between the quark- and gluon- jets are observed. Our method complements the usual studies of quark- and gluon- jet differences since no jet tagging is used. A change of jet properties with jet energy is also observed. However, comparison of the results from the two topologies suggests that the jet environment, dependent on the event topology, plays a role in determining the jet properties as well as the jet energy.

Appendix - Data Selection

The following cuts were used in the selection of the data used in this report.

Number of GOOD (defined below) charged tracks	>4
Total charged energy	>0.15 $\sqrt{s}$
angle of the sphericity axis to the beam line	> 30°
GOOD tracks are defined as follows	
distance to the primary vertex in x- y projection	<3.0 cm
distance to the primary vertex in z- projection	<5.0 cm
momentum transverse to beam line	>0.2 GeV/c
angle between track momentum and the beam line	>20°
number of TPC co-ordinates	>4

In addition clusters of energy greater than 0.2 GeV detected in the ECAL or HCAL which were unassociated with charged tracks were included in the jet finding procedure.

After jet finding the following additional cuts were applied	
angle between each jet axis and the beam line	>30°
number of particles in each jet	>2
sum of angles between jet axes, $\psi_1 + \psi_2 + \psi_3$	>359°
jet energies, $\left\|(E_i^{calc} - E_i^{vis}) / E_i^{calc}\right\|$ i=1,3	<0.5

E^{vis} is the visible jet energy and E^{calc} is the jet energy calculated from the inter- jet angles (see section **Jet Topologies**).

Appendix - Likelihood Function

The Likelihood function given in the section **Analysis Method** is obtained as follows from the expected contents of the scatter plot n_{ij}. The probability of observing D events where n are expected is

$$p = e^{-n} \frac{n^D}{D!}$$

The maximum likelihood method then attempts to maximise the product of probabilities over all bins, or equivalently, $L = \sum \ln p$, which becomes

$$L = \sum D \ln n - \sum n - \sum \ln(D!)$$

Since our expression for n_{ij} is such that $\sum n$ is independent of the parameters, then we only need to consider the first term in the above expression. Further, since n is given by

$$n_{ij} = (s_i s_j - d_i d_j) / 2N$$

or

$$n_{ij} = \frac{s_i s_j}{2N} \left(1. - \frac{d_i d_j}{s_i s_j} \right)$$

and since the s_i and N are constants, we can finally write the likelihood function as

$$L = \sum_{ij} D_{ij} \ln \left(1. - \frac{d_i d_j}{s_i s_j} \right)$$

Mean Values of Distributions of Figures 1 - 5.

(quark / gluon / ratio : statistical errors only)

	150° sample 1992	150° sample 1993	120° sample 1992 + 1993	high energy quark jet 1992
Energy Range (GeV) Mean Energy (GeV) Number of Events	20 - 29 24.4 11933	20 - 29 24.4 10651	26 - 35 30.4 3982	39.5 - 44.5 42.6 11933
Charged Particle Multiplicity	6.33 ± .09 7.73 ± .11 (1.22 ± .03)	6.52 ± .13 7.47 ± .13 (1.14 ± .04)	7.22 ± .11 9.05 ± .25 (1.25 ± .05)	8.07 ± .03
Fraction of Jet Energy in cone of semi-angle of 10°	0.583 ± .005 0.411 ± .004 (0.70 ± .01)	0.574 ± .005 0.419 ± .004 (0.73 ± .01)	0.564 ± .017 0.440 ± .033 (0.78 ± .08)	0.711 ± .002
$\sum\|p_t\|$ for all particles of Jet (GeV)	4.71 ± .05 6.28 ± .04 (1.33 ± .02)	4.92 ± .05 6.14 ± .04 (1.25 ± .02)	5.87 ± .19 7.91 ± .39 (1.34 ± .10)	6.54 ± .03
Jet Mass (GeV/c^2)	6.39 ± .04 8.28 ± .04 (1.30 ± .01)	6.62 ± .05 8.15 ± .04 (1.23 ± .02)	8.12 ± .10 10.87 ± .24 (1.34 ± .04)	10.17 ± .03
Leading X_E (charged particles)	0.245 ± .004 0.220 ± .004 (0.90 ± .03)	0.247 ± .004 0.217 ± .004 (0.88 ± .03)	0.239 ± .006 0.208 ± .012 (0.87 ± .07)	0.247 ± .001
Total Particle Multiplicity	13.36 ± .10 15.20 ± .10 (1.14 ± .02)	14.00 ± .09 14.77 ± .10 (1.05 ± .02)	14.96 ± .36 18.05 ± .69 (1.21 ± .07)	16.83 ± .05

Energy Distribution within Quark- and Gluon-Jets

The following tables show the mean fraction of energy (charged + neutral particles) within cones of given semi- angle.

A. $22.5 < E_{jet} < 27$ GeV from 1992 + 1993 data (10938 events).

Cone semi- angle (degrees)	Mean fraction of energy in cone	
	Quark Jet	Gluon Jet
5°	0.302(5)	0.176(5)
10°	0.577(5)	0.417(5)
15°	0.731(4)	0.602(4)
20°	0.815(4)	0.740(4)
25°	0.868(4)	0.837(4)
30°	0.914(3)	0.886(3)

B. $39.5 < E_{jet} < 44.5$ GeV from 1992 data (11933 events).

Cone semi- angle (degrees)	Mean fraction of energy in cone. Quark Jet
5°	0.445(3)
10°	0.711(2)
15°	0.827(2)
20°	0.883(1)
25°	0.915(1)
30°	0.935(1)

The errors shown are statistical only.

Figure Captions

Figures 1.1 to 5.6 are all normalised plots of $\frac{1}{N}\frac{dN}{dV}$, where V is a jet variable (such as charged multiplicity) specified by the second digit of the figure number (after the point). The first digit specifies the data sample which is described in detail in section **Jet Topologies** and summarised below. The quark- and gluon-distributions are indicated by the data points marked by ■ and ● respectively.

The jet variables shown in the figures (from top left in usual order) are

.1 Charged particle multiplicity of jet.

.2 $X_E = E_{particle} / E_{jet}$ for leading charged particle in jet.

.3 Total particle multiplicity of jet

.4 Total transverse momentum of jet, $\sum P_t$, where P_t is the component of particle momentum transverse to the jet axis. Both charged and neutral particles are included.

.5 Fraction of jet energy (charged and neutral) within a cone of semi- angle 10° centred about the jet axis.

.6 Jet mass (GeV/c²)

The data sets used are specified by the first digit as follows;

1. 1992 data, $20 < E_{jet} < 29$ GeV.

2. 1993 data, $20 < E_{jet} < 29$ GeV.

3. 1992 + 1993 data, $22.5 < E_{jet} < 27$ GeV.

4. 1992 + 1993 data, $26 < E_{jet} < 35$ GeV. This data is the only use of the 120° (mercedes) sample.

5. 1992 data, $39.5 < E_{jet} < 44.5$ GeV. The high energy jet of the 150° sample gives only the quark- distribution.

6. The folded Dalitz plot of x_2 versus x_3 ($x_1 > x_2 > x_3$) showing the regions of the 150° and 120° (mercedes) data samples determined by angle and weak energy cuts. The positions of the additional tighter energy cuts for the 150° sample are also shown.

7. The fraction of jet energy (charged and neutral) within cones of semi- angle of 5, 10, 15, 20, 25, and 30 degrees respectively (figures 7.1 - 7.6) for 92 + 93 150° data with tight energy cut, $\overline{E}$ = 24.5 GeV.

8. As figure 7 for data sample 5. : high energy quark- jets. $\overline{E}$ = 42.6 GeV.

9. (a) The mean jet energy within cones of varying semi- angle obtained from the data of figures 7 and 8 (see also table 2): gluon and quark data for mean jet energy of 24.5 GeV., solid circles and squares respectively; quark data for mean jet energy of 42.6 GeV., open squares. Statistical errors are smaller than the data points. (b) Modified from original of A. Moutoussi. - see LAPP/annecy meeting 94. The data for the low energy jets of the two 150° sample results are in complete agreement.

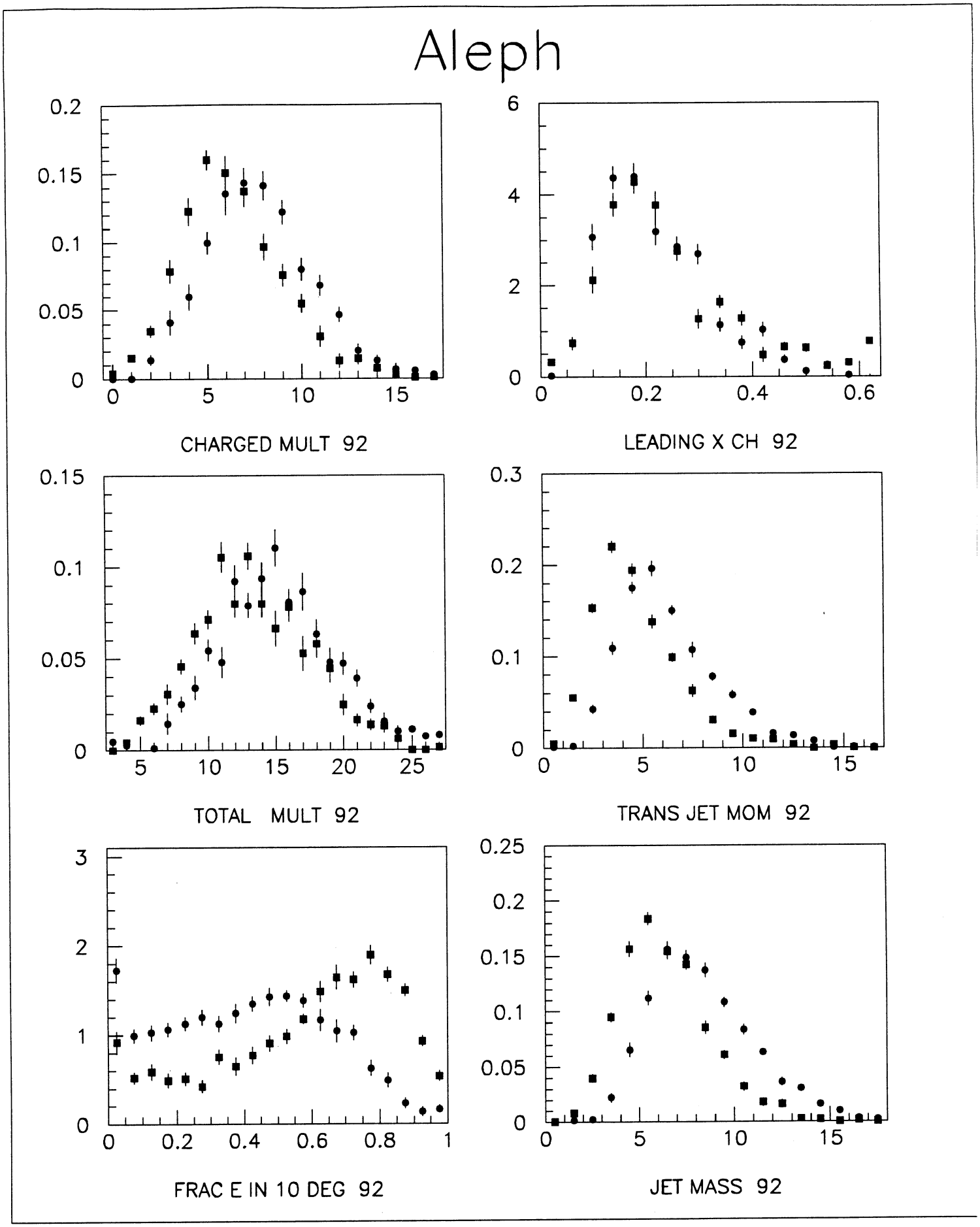
Aleph
CHARGED MULT 92
LEADING X CH 92
TOTAL MULT 92
TRANS JET MOM 92
FRAC E IN 10 DEG 92
JET MASS 92

Fig 1.

Aleph

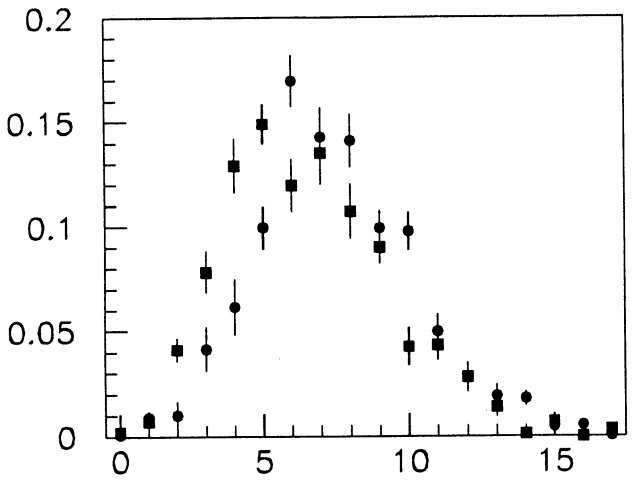

CHARGED MULT 93

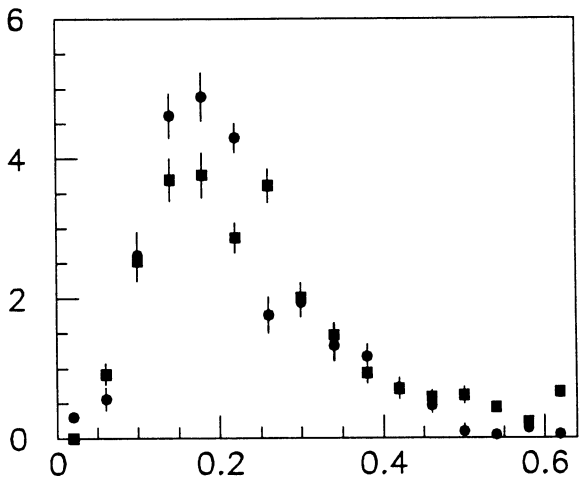

LEADING X CH 93

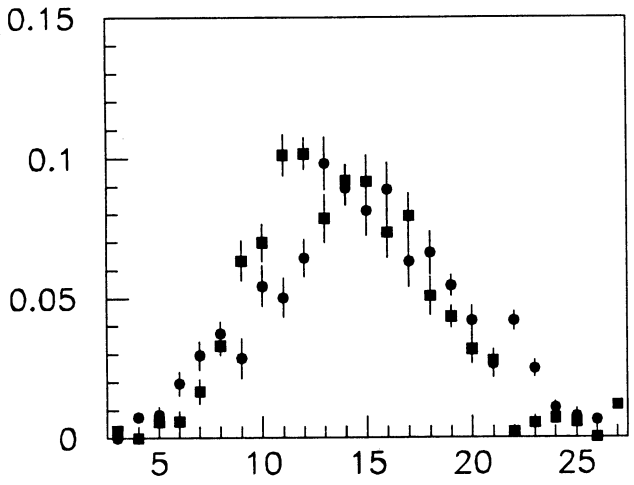

TOTAL MULT 93

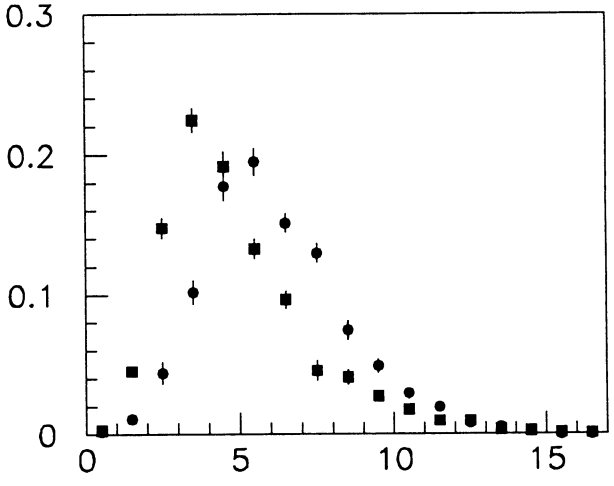

TRANS JET MOM 93

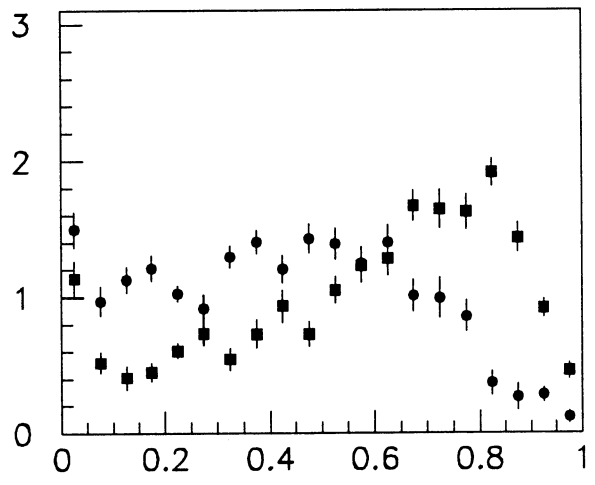

FRAC E IN 10 DEG 93

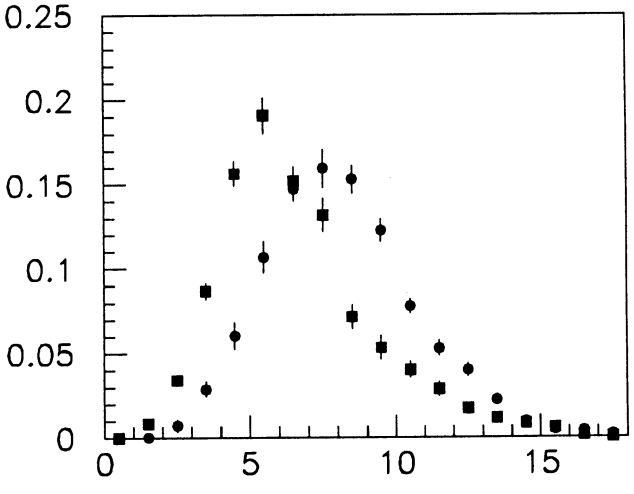

JET MASS 93

Fig 2

Aleph

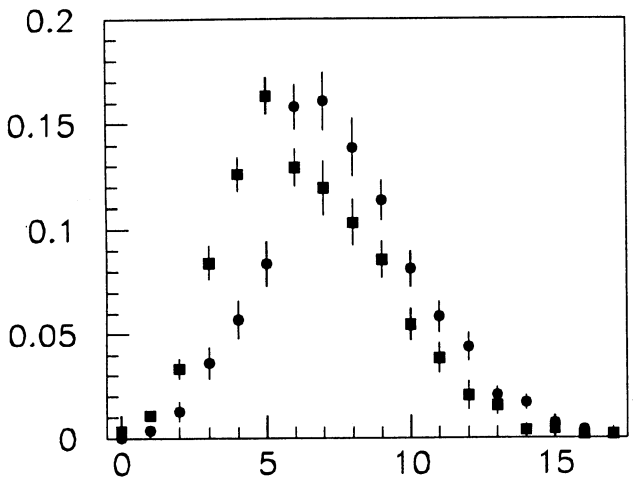

CHARGED MULT 92/93

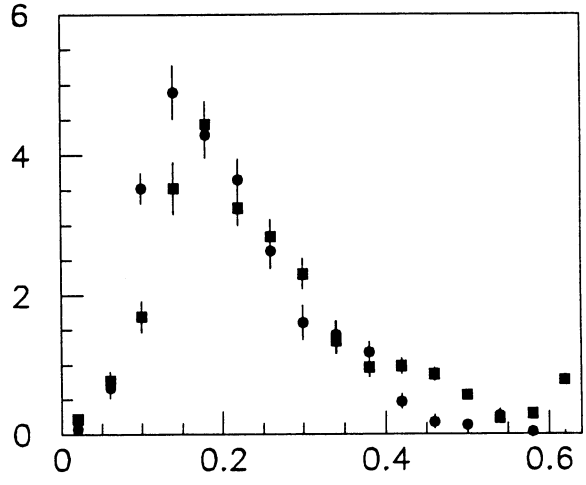

LEADING X CH 92/93

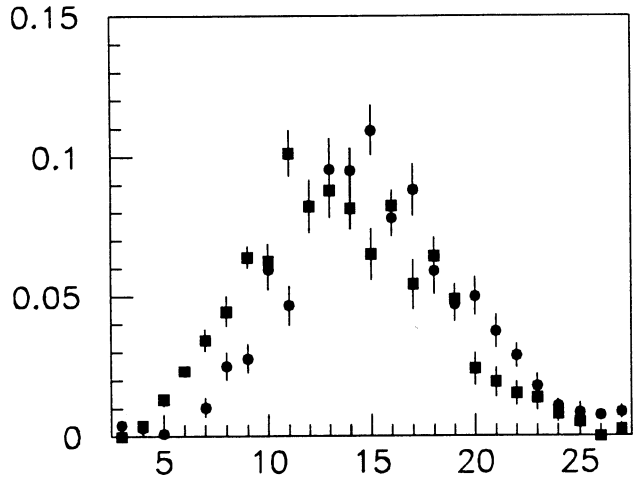

TOTAL MULT 92/93

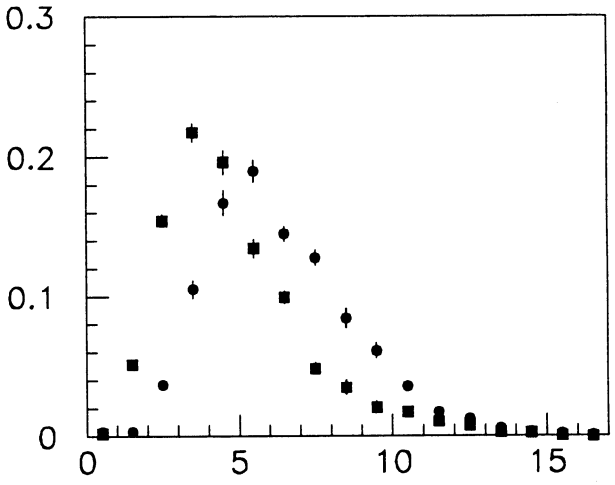

TRANS JET MOM 92/93

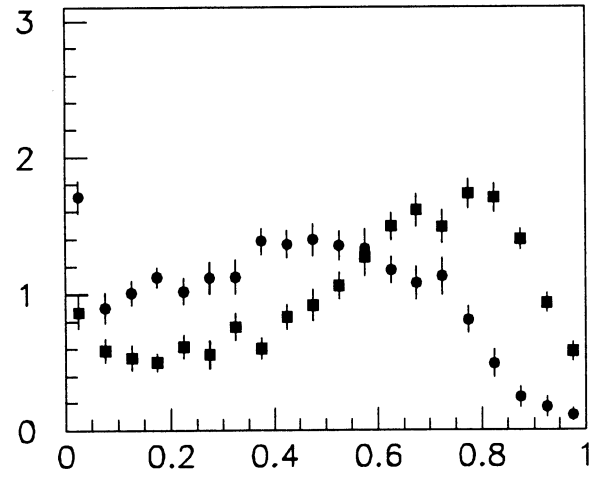

FRAC E /10 DEG 92/93

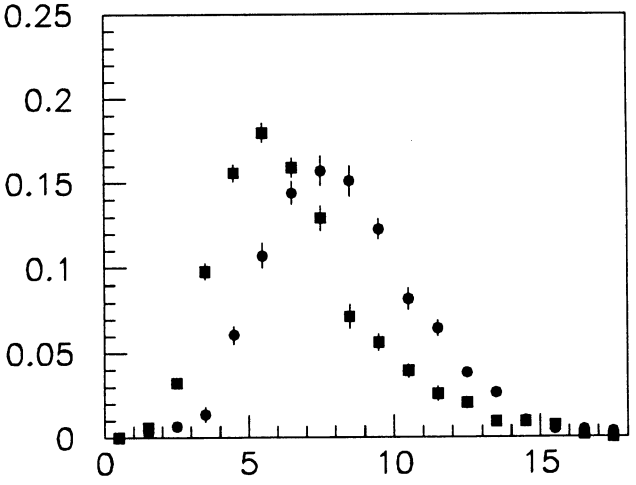

JET MASS 92/93

Fig 3

Aleph

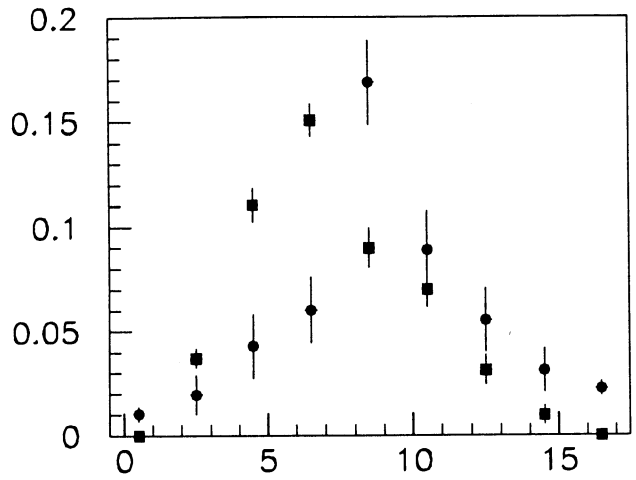

CHARGED MULT 120

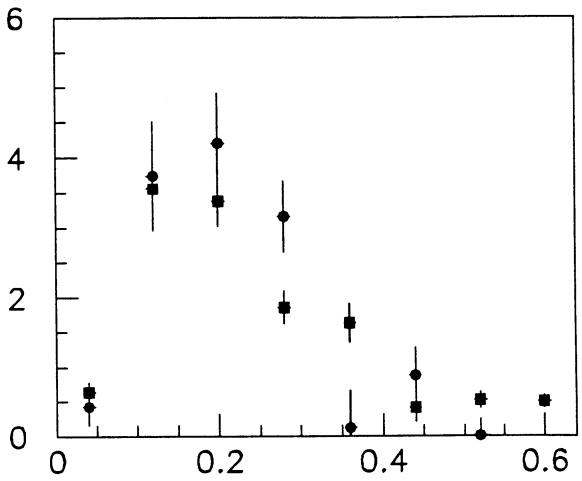

LEADING X CH 120

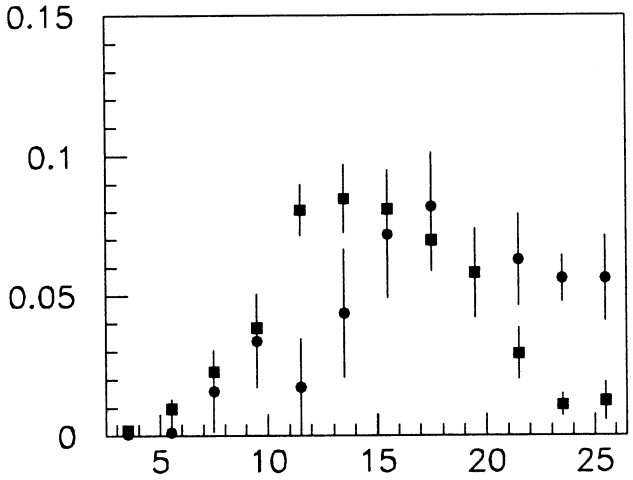

TOTAL MULT 120

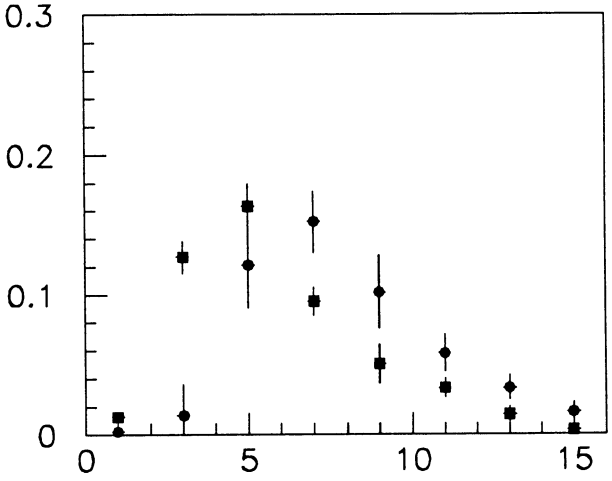

TRANS JET MOM 120

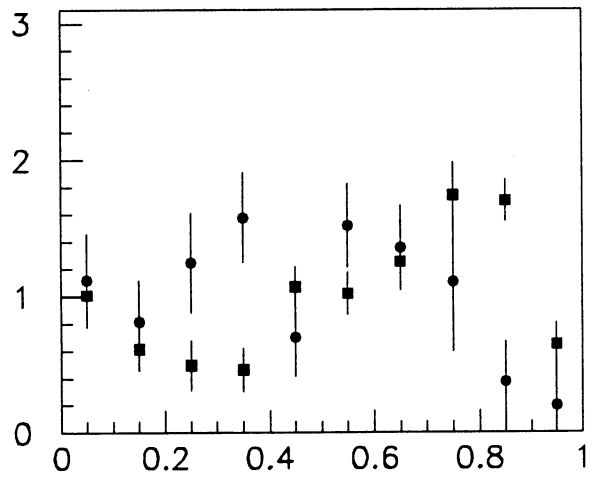

FRAC E IN 10 DEG.120

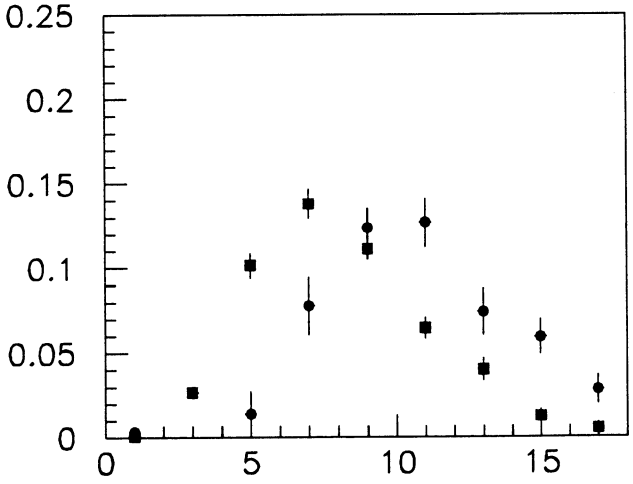

JET MASS 120

Fig 4

Aleph

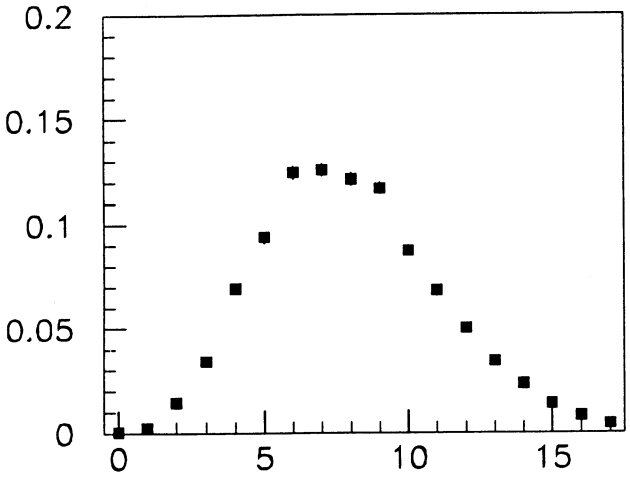

JET CH MULTIPLICITY

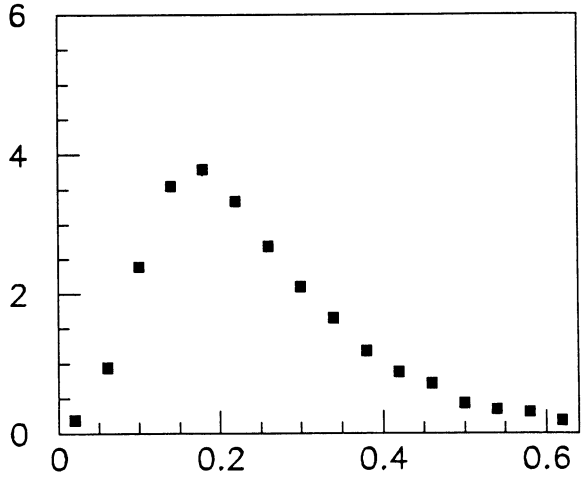

JET LEADING CH E/EJ

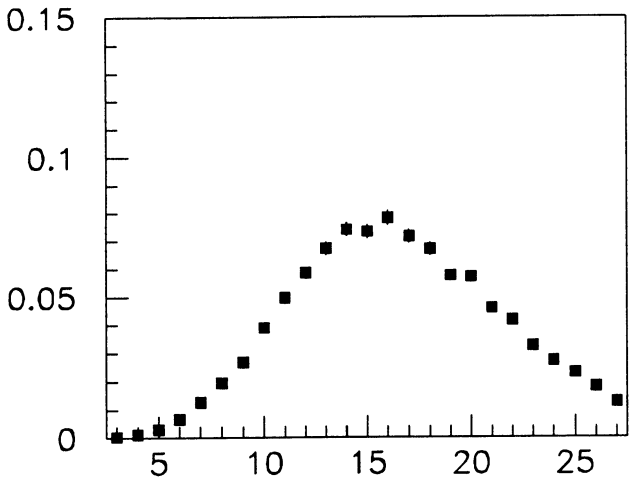

JET TOT MULTIPLICIT

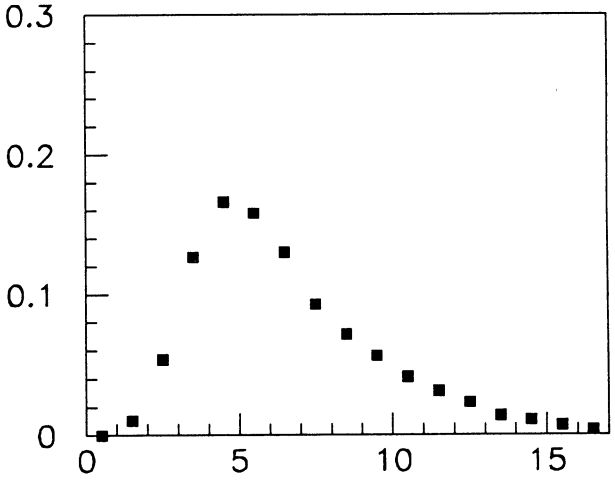

TRANSVERSE JET MOME

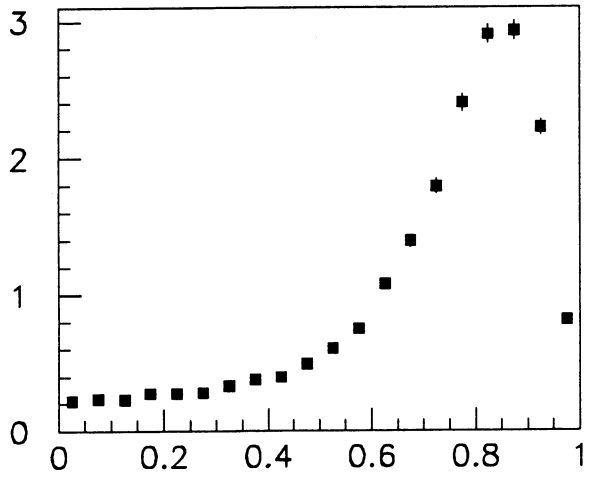

ENERGY FRAC/ 10 DEG

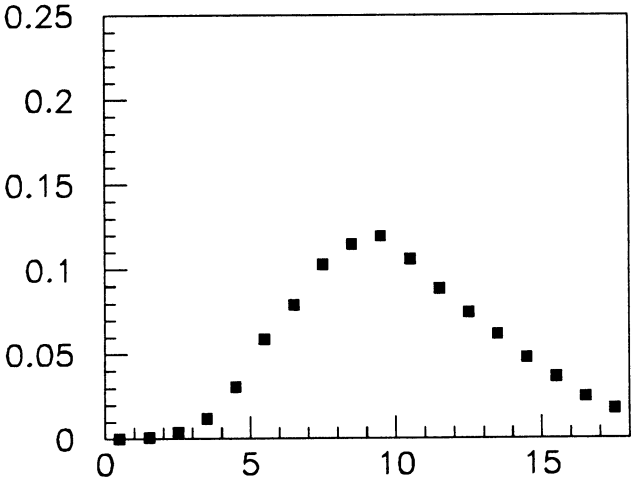

JET MASS

Fig 5

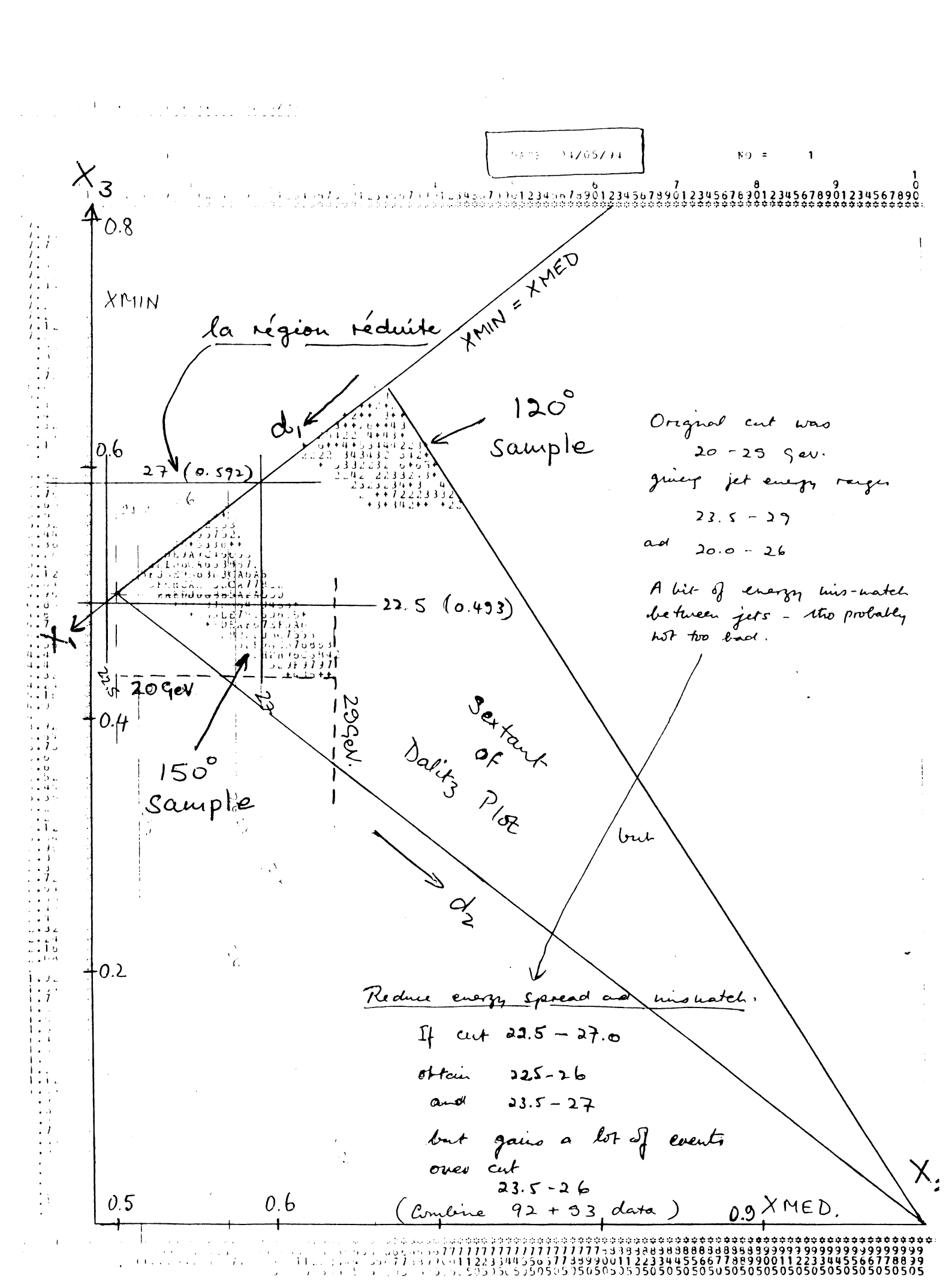

Original cut was
20 - 25 GeV.
giving jet energy ranges
23.5 - 29
and 20.0 - 26

A bit of energy mis-match between jets - this probably not too bad.

but

Reduce energy spread and mismatch.

If cut 22.5 - 27.0
obtain 22.5 - 26
and 23.5 - 27
but gains a lot of events over cut
23.5 - 26
(Combine 92 + 93 data)

Fig 6

Aleph

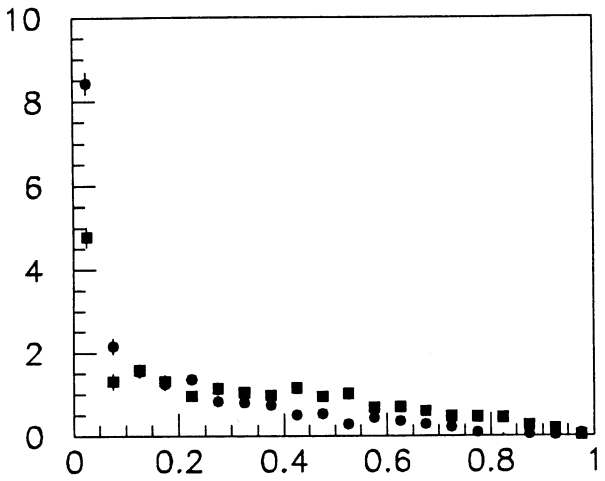

FRAC E / 5 DEG 92/93

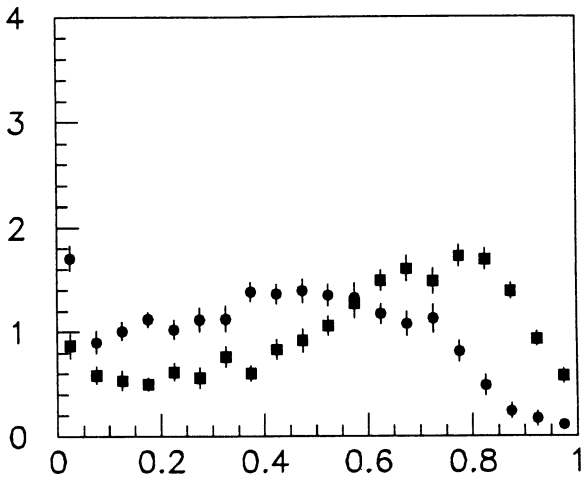

FRAC E /10 DEG 92/93

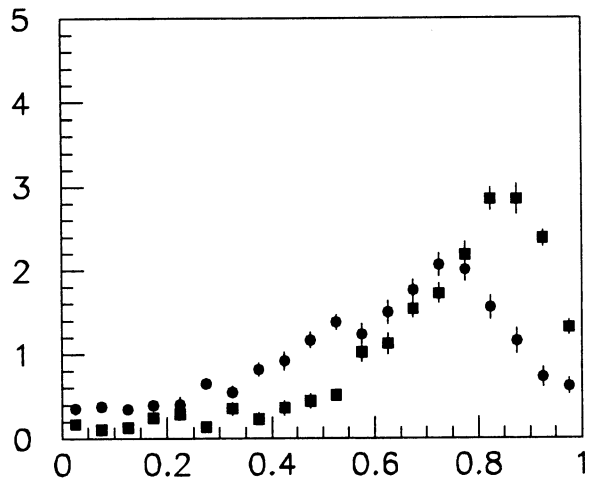

FRAC E/15 DEG 92/93

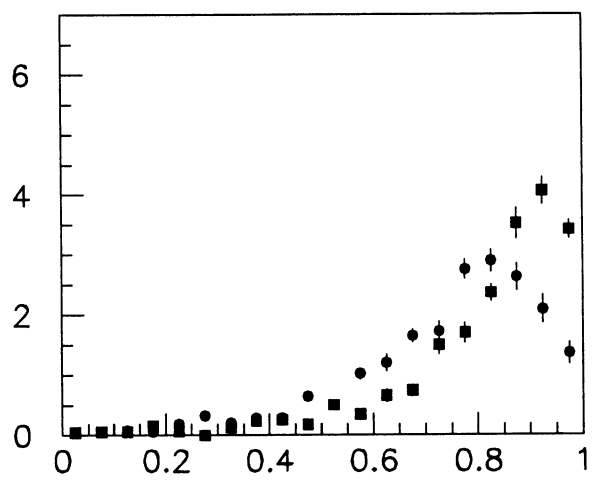

FRAC E/20 DEG 92/93

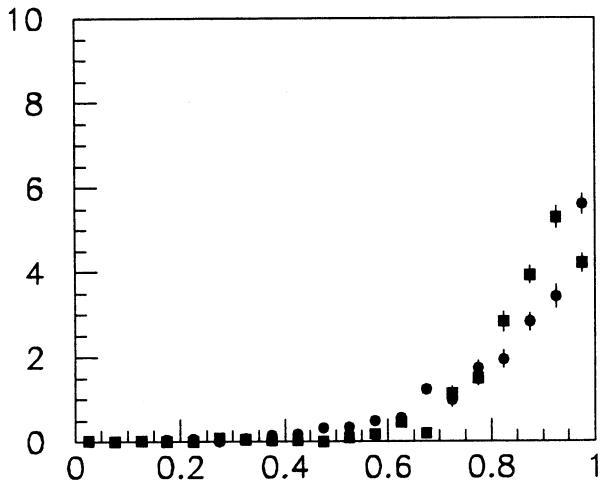

FRAC E/ 25 DEG 92/93

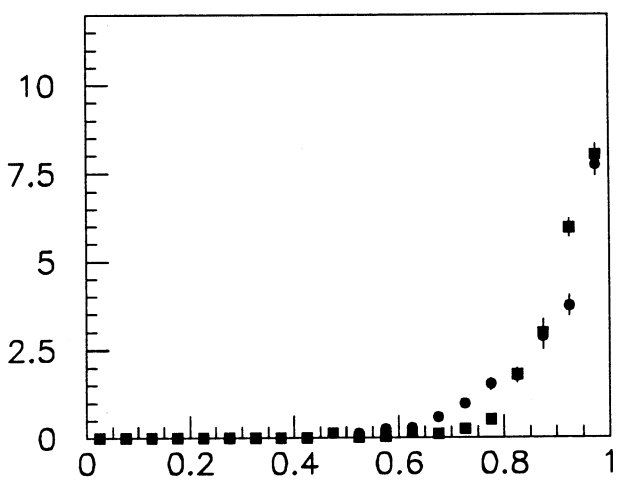

FRAC E/ 30 DEG 92/93

Fig 7

Aleph

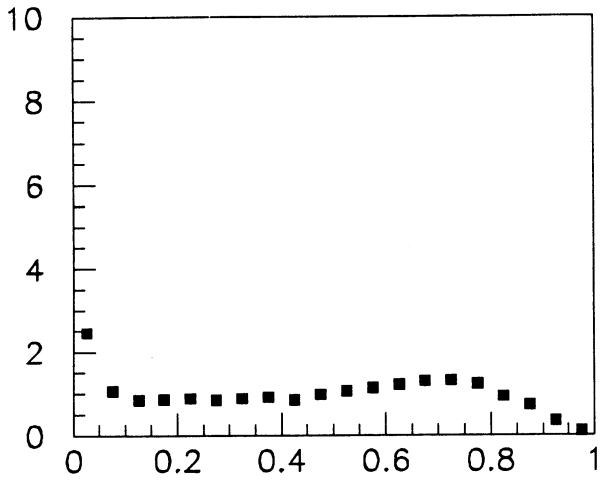

ENERGY FRAC 05 DEG

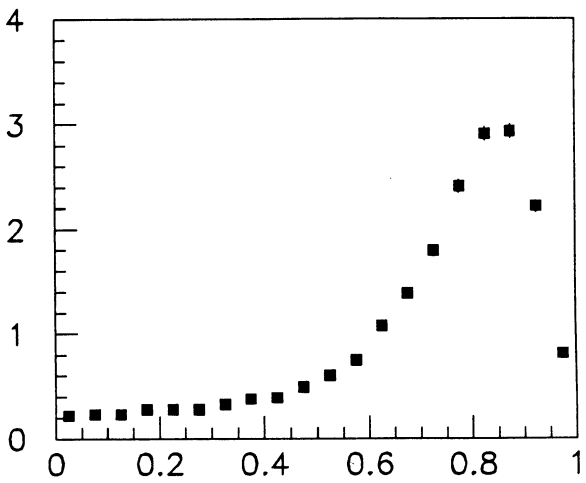

ENERGY FRAC 10 DEG

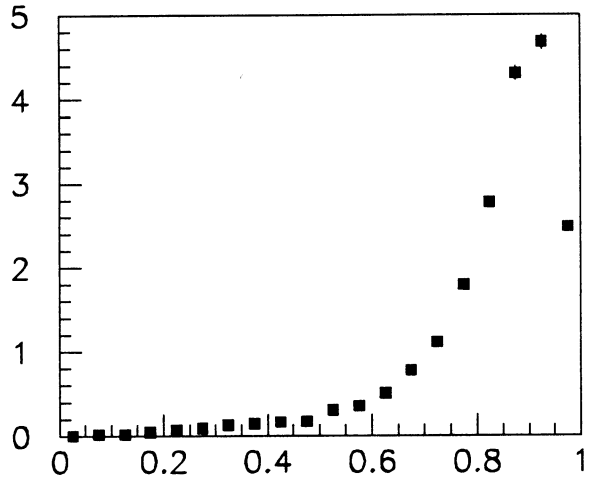

ENERGY FRAC 15 DEG

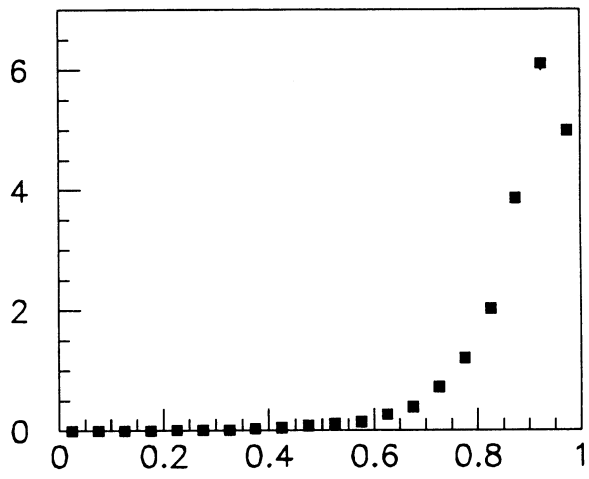

ENERGY FRAC 20 DEG

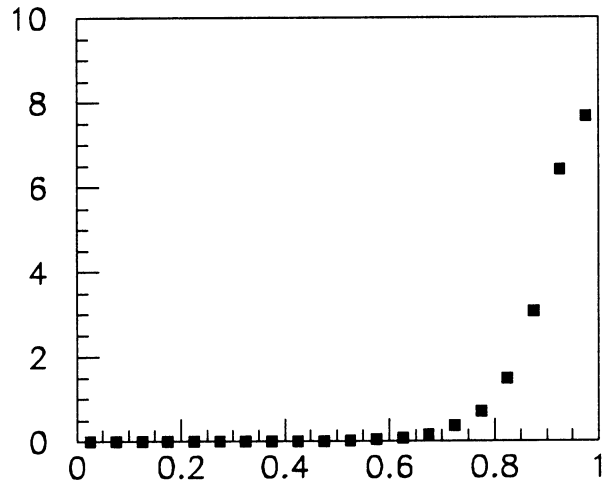

ENERGY FRAC 25 DEG

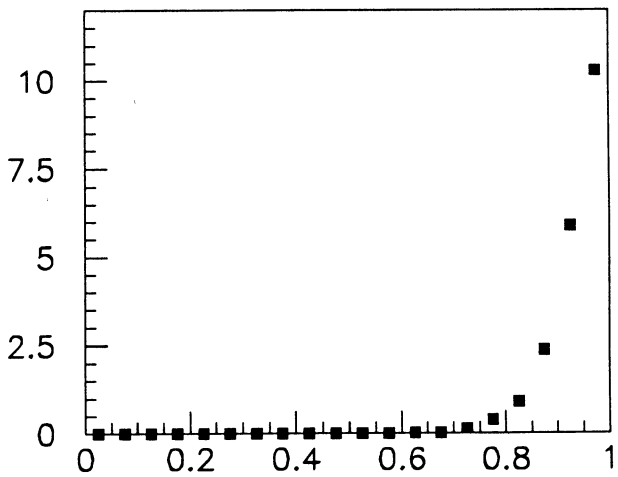

ENERGY FRAC 30 DEG

Fig 8

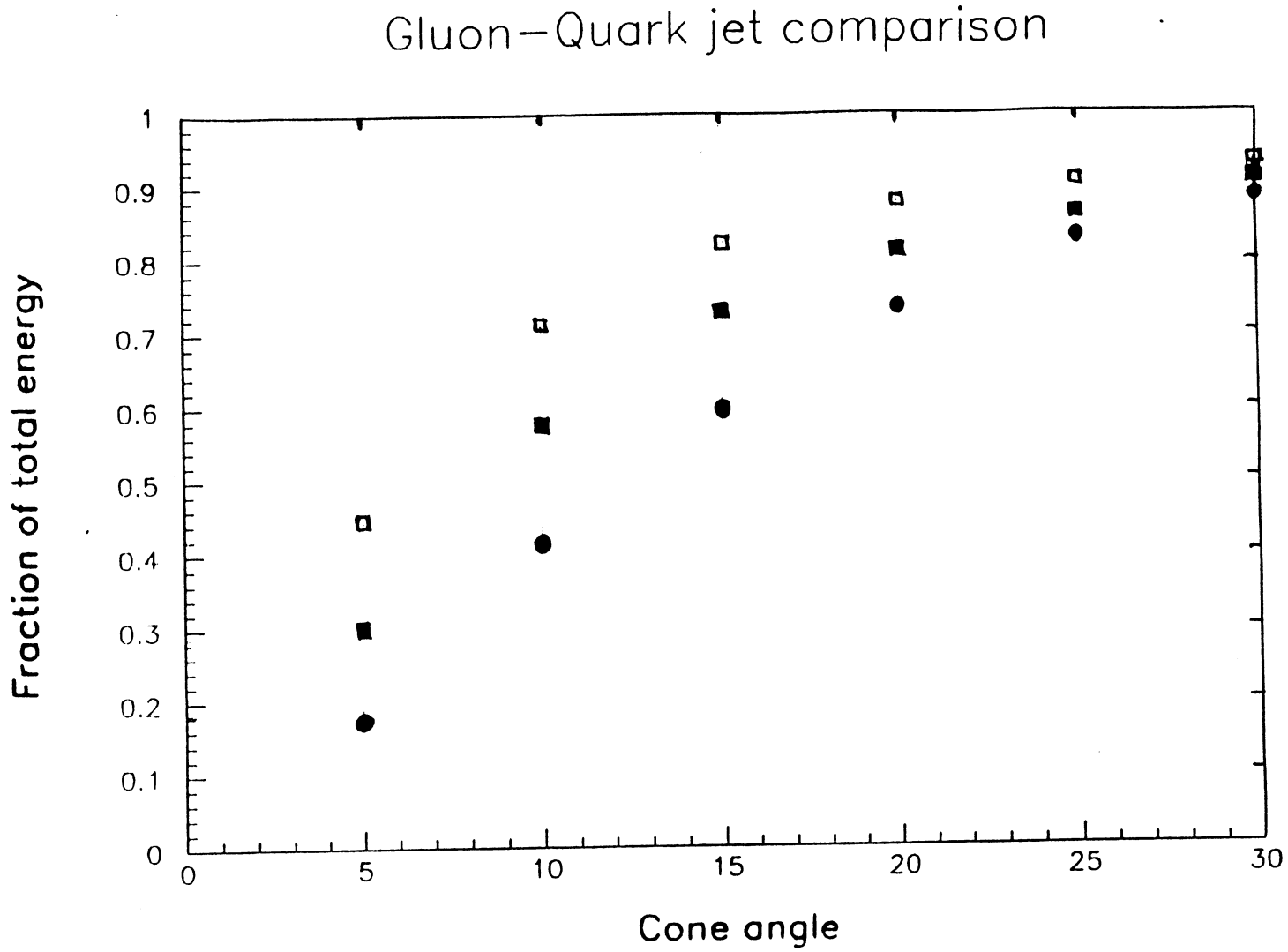
Gluon–Quark jet comparison
Fraction of total energy
Cone angle
0
0.1
0.2
0.3
0.4
0.5
0.6
0.7
0.8
0.9
1
0
5
10
15
20
25
30

Figure 9a.

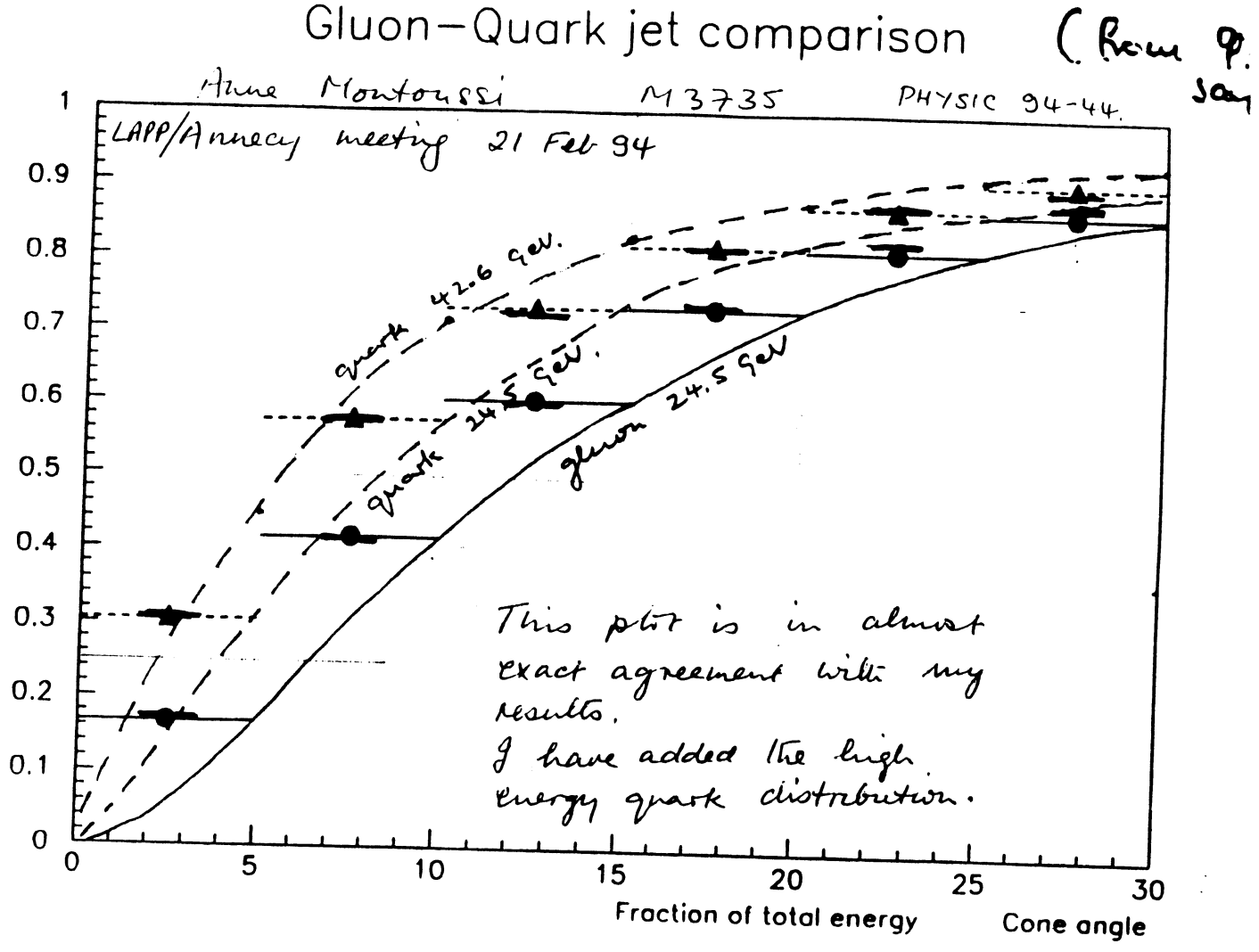

Short bars — are from M. Scarr same topology, same bin sizes,

Fig 9b